

# The coulometric approach to the superoxide scavenging activity determination: The case of porphyrin derivatives influence on oxygen electroreduction

Sergey M. Kuzmin\*, Svetlana A. Chulovskaya and Vladimir I. Parfenyuk<sup>◇</sup>

G.A. Krestov Institute of Solution Chemistry of the Russian Academy of Sciences, Ivanovo 153045, Russia

Received 12 May 2015

Accepted 4 July 2015

**ABSTRACT:** The electrochemical and antioxidant properties of 5,10,15,20-tetrakis(3'-hydroxyphenyl) porphyrin ( $H_2T(m\text{-OHP}h)P$ ) and 5,10,15,20-tetrakis(4'-hydroxyphenyl)porphyrin ( $H_2T(p\text{-OHP}h)P$ ) were tested by the cyclic voltammetry (CV) method. It is shown that in dimethylsulfoxide (DMSO) the electroreduction processes of oxygen and porphyrins are under diffusion control. The electroreduction of  $H_2T(m\text{-OHP}h)P$  and  $H_2T(p\text{-OHP}h)P$  with potentials about -1 V are irreversible due to the chemical step (EC process) which leads to products with oxidation potentials about -0.5 V. Additionally in case of oxygen and porphyrin coreduction, both  $H_2T(m\text{-OHP}h)P$  and  $H_2T(p\text{-OHP}h)P$  influence the  $O_2^{\cdot -}$  electrosynthesis. The nonlinear dependence of the  $O_2^{\cdot -}$  peak current vs. porphyrin concentrations makes the available amperometric approach unsuitable for antioxidant activity estimation. To solve this problem, the coulometric parameters were calculated. The excellent linearity of the coulometric response of superoxide ion vs. porphyrins concentration was demonstrated for a wide concentration range. On the basis of coulometric responses, we constructed a parameter which separated the radical scavenging activity and variation of oxygen electroreduction. The superoxide scavenging activities of  $H_2T(m\text{-OHP}h)P$  and  $H_2T(p\text{-OHP}h)P$  were determined using the developed approach. The effect of OH group position on the superoxide scavenge activity is shown:  $H_2T(p\text{-OHP}h)P$  has a higher activity (slope = 0.75 L.mmol<sup>-1</sup>) than  $H_2T(m\text{-OHP}h)P$  (slope = 0.60 L.mmol<sup>-1</sup>).

**KEYWORDS:** porphyrin, cyclic voltammetry, coulometric approach, superoxide scavenging activity.

## INTRODUCTION

Free radicals are a special class of chemicals which have an unpaired electron. As a rule, they are aggressive oxidants which lead to pathologies of biochemical processes and damage of cells, especially cell membranes. Different antioxidants prevent the damaging effects of free radicals on living cells [1, 2]. It is known that heterocyclic compounds [3, 4] and some porphyrin ligands [5, 6] have a significant antioxidant activity. The complexes of porphyrins with transition metals exhibit superoxide scavenging activity and are promising for pharmaceutical

applications [7, 8]. The phenolic fragments with a labile hydrogen atom in the porphyrins leads to the detection of antioxidant properties [9]. However, the porphyrin structure impact on the activity and mechanisms of antioxidant action are insufficiently studied up to now. The high absorption coefficients of porphyrins [10] lead to difficulties in spectrometric measurements [11] of antioxidant activity. Therefore, the electrochemical assay was preferred. The determination of radical scavenging properties of compounds is based on the monitoring of superoxide amperometric response in the antioxidant presence [12–16]. Previously [17], we have shown the antioxidant properties of 5,10,15,20-tetrakis(4'-aminophenyl)porphyrin and the essential influence of the substituent position on the superoxide scavenging activity. This paper is focused on the development of

<sup>◇</sup> SPP full member in good standing

\*Correspondence to: Sergey M. Kuzmin, email: smk@isc-ras.ru, tel: +7 915-824-9554

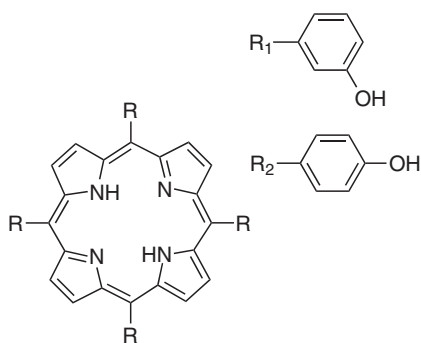


Fig. 1. Chemical structures of porphyrins

a coulometric approach to the superoxide scavenging activity determination in case of antioxidants influence on the superoxide electro-synthesis process.

## EXPERIMENTAL

### Procedure of synthesis

$H_2T(m\text{-OHPh})P$  and  $H_2T(p\text{-OHPh})P$  (Fig. 1) were synthesized by the two-step method [18, 19] via demethylation of methoxyphenylporphyrins that was obtained in high yield by condensation of benzaldehydes with pyrrole [20]. The purified products were characterized by thin-layer chromatography (silufol plates), UV-vis spectrometry (Varian Cary 50 spectrometer) and  $^1H$  NMR spectrometry (Bruker AVANCE-500 spectrometer) methods.

**5,10,15,20-Tetrakis(3'-methoxyphenyl)porphine {intermediate compound}.** A solution of 5.4 g (0.04 mol) of 3-methoxybenzaldehyde and 2.7 mL (0.04 mol) pyrrole in 50 mL xylene was drop added to a boiling solution of 5.0 g of chloroacetic acid in 150 mL of a mixture of isomeric xylenes during 20 min. The resulting mixture was refluxed with air bubbling for one additional hour. After that, xylene was steamed, the deposit was filtered off, washed with water and dried in air at 70 °C. The deposit was dissolved in chloroform and purified on aluminum oxide (Brockmann Activity III) eluting with chloroform. The first red zone was collected, the eluate was evaporated, and the porphyrin was precipitated with methanol, filtered and dried at room temperature in air. The yield was 2.0 g (27.2%).  $R_f = 0.45$  ( $CHCl_3$  — hexane, 1:1).  $^1H$  NMR (500 MHz,  $CDCl_3$ ,  $Me_4Si$ ):  $\delta_H$ , ppm -2.85 s (2H, s, pyrrole-NH), 3.92 (12H, s, -O- $CH_3$ ), 7.28, 7.53 and 7.71 (16H, m, H-Ph), 8.85 (8H, s, pyrrole-H). UV-vis ( $CHCl_3$ ):  $\lambda_{max}$ , nm (log  $\epsilon$ ) 648 (3.72), 590 (3.83), 550 (3.89), 516 (4.31), 420 (5.70).

**5,10,15,20-Tetrakis(3'-hydroxyphenyl)porphine.** 4.5 g of boron tribromide was added to 1.5 g (2.04 mmol) of 5,10,15,20-tetrakis(3'-methoxyphenyl)porphyrin solution being stirred and cooled in 50 mL of dry chloroform.

The mixture was stirred at room temperature for 2 h, and then 5 mL of methanol was added. Fifteen minutes later, 2.5 mL of ammonia solution was drop added until the color changed from green to red. Chloroform was distilled off, the residue dried, dissolved in 5% potassium hydroxide solution, filtered and precipitated by diluted hydrochloric acid. The precipitate was filtered off, washed with water and dried in air at room temperature. The deposit was dissolved in ethyl acetate and purified on silica gel by eluting with ethyl acetate. The eluate was evaporated and precipitated with petroleum ether. Yield 1.35 g (97.5%).  $R_f = 0.88$  (ethyl acetate).  $^1H$  NMR (500 MHz,  $CDCl_3$ ,  $Me_4Si$ ):  $\delta_H$ , ppm -2.45 (2H, s, pyrrole-NH), 7.33 and 7.85 (16H, m, H-Ph), 8.52 (8H, s, pyrrole-H). UV-vis ( $CHCl_3$ ):  $\lambda_{max}$ , nm (log  $\epsilon$ ) 645 (3.71), 588 (3.88), 550 (3.92), 514 (4.31), 419 (5.62).

**5,10,15,20-Tetrakis(4'-methoxyphenyl)porphine {intermediate compound}.** A solution of 5.0 mL (72.2 mmol) of pyrrole and 8.8 mL (72.2 mmol) of anisaldehyde was drop added to a boiling solution of 16 g of chloroacetic acid in 300 mL of an isomeric xylenes mixture for 20 min. The resulting mixture was refluxed with air bubbling for one more hour. After xylene steaming, the deposit was filtered off, washed with water and dried in air at 80 °C. The deposit was dissolved in chloroform and purified on aluminum oxide (Brockmann Activity III) eluting with chloroform. The first red zone was collected, the eluate was evaporated, and the porphyrin was precipitated with methanol, filtered and dried at room temperature in air. The yield was 5.6 g (42%).  $R_f = 0.33$  ( $CHCl_3$ ).  $^1H$  NMR (500 MHz,  $CDCl_3$ ,  $Me_4Si$ ):  $\delta_H$ , ppm -2.79 (2H, s, pyrrole-NH), 4.03 (12H, s, -O- $CH_3$ ), 7.22 (8H, d, m-H-Ph), 8.06 (8H, d, o-H-Ph), 8.79 (8H, s, pyrrole-H 8H). UV-vis ( $CHCl_3$ ):  $\lambda_{max}$ , nm (log  $\epsilon$ ) 652 (3.87), 595 (3.78), 557 (4.07), 520 (4.25), 423 (5.69).

**5,10,15,20-Tetrakis(4'-hydroxyphenyl)porphine.** A solution of 0.5 mL (5.29 mmol) of boron tribromide in 10 mL of methylene chloride was added to the stirring and cooling solution of 1.0 g (1.36 mmol) of 5,10,15,20-tetrakis(4'-methoxyphenyl)porphyrin in 200 mL of dried methylene chloride. The mixture was stirred at room temperature for 2 h, and then 5 mL of methanol was added. The mixture was neutralized by ammonia until the color changed from green to dark cherry, washed with water, dried over sodium sulfate and evaporated to dryness. The deposit was dissolved in ethyl acetate and purified on silica gel by eluting with ethyl acetate. The eluate was evaporated and precipitated with petroleum ether. Yield 0.9 g (98%).  $R_f = 0.33$  ( $CHCl_3$ ).  $^1H$  NMR (500 MHz;  $CDCl_3$ ,  $Me_4Si$ ):  $\delta_H$ , ppm -2.92 (2H, s, pyrrole-NH), 7.70 (8H, d, m-H-Ph), 8.08 (8H, d, o-H-Ph), 8.79 (8H, s, pyrrole-H). UV-vis ( $CHCl_3$ ):  $\lambda_{max}$ , nm (log  $\epsilon$ ) 650 (3.72), 595 (3.71), 556 (3.90), 519 (4.06), 423 (5.43).

The porphyrins characterized by standard analytical and spectroscopic techniques agree quite well with the reported data [21, 22].

## Electrochemical procedure

Intensity and position of UV-vis absorption bands did not change in the presence of supported electrolyte, which indicates that there was no interaction between the ions of the supported electrolyte and the studied porphyrins.

Dimethylsulfoxide (DMSO  $\geq 99.5$ , ALDRICH) was purified by the zone melting method and then stored over molecular sieves in a dry box before use. Tetrabutylammonium perchlorate (TBAP  $\geq 98.0$ , ALDRICH) was purified by recrystallization from ethanol. The concentrated solutions of porphyrins containing 0.02 M TBAP were prepared as supported electrolyte by the gravimetric method using electronic analytical balance «Sartorius» ME215S. The lower concentrations of porphyrins were prepared by serial dilutions. DMSO was selected as the solvent in electrochemical studies because porphyrins are readily soluble in the solvent,  $O_2^{\bullet -}$  is stable and can be electrochemically generated.

The electrochemical cell and measurement procedure are described elsewhere [6, 17]. The cell was a temperature-controlled ( $25 \pm 0.5^\circ\text{C}$ ) vessel which was separated by a porous glass plug into two volumes to segregate the working and auxiliary electrodes. The saturated calomel electrode (SCE) inserted into the electrochemical cell through the Luggin capillary was used as the reference electrode. Before measuring, the working electrode (the polishing platinum strip with an active area of  $1.2\text{ cm}^2$ ) was pretreated by mechanical polishing, degreased with ethanol, and etched by a chromic mixture for 20 min, carefully washed out by distilled water and test solution. The working electrode was immersed in the cell with the test solution where the potential of the working electrode reached a steady value in 10 min. The atmospheric pressure of argon or oxygen was used for solution degassing or oxygenation. The oxygen saturation condition was verified using the cyclic voltammetry (CV) method. In this case, the dissolved oxygen concentration

equals 2.1 mM [23, 24]. A free convection mode was formed within 3 min after removing the capillary from the solution. Thereafter the first cycles of voltammograms were recorded at scan rates from 0.005 to 1 V/sec. The CV data were corrected for Ohmic ( $iR$ ) losses using a current interruption technique [25].

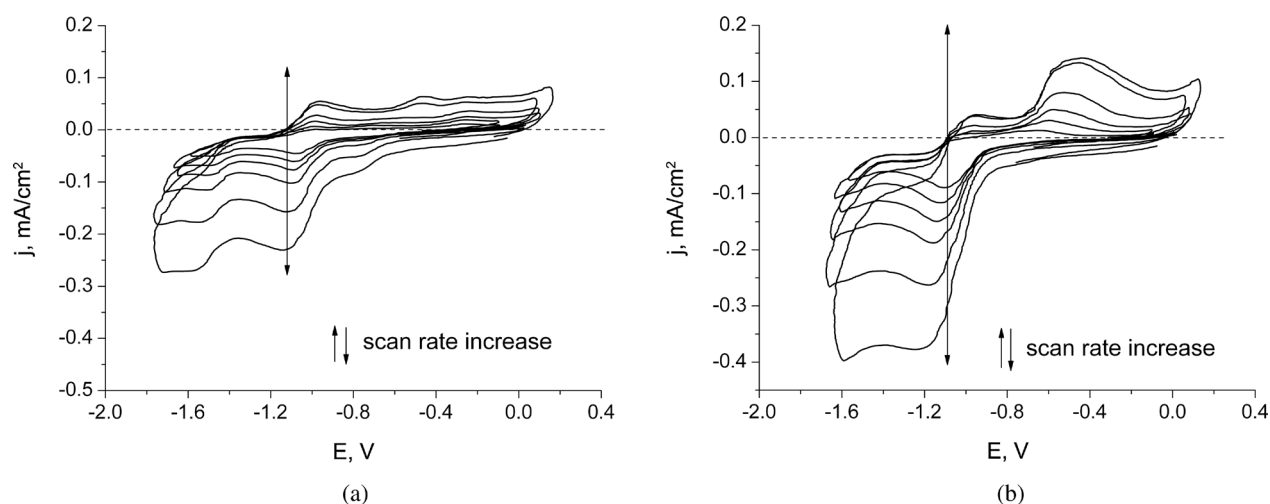
## RESULTS AND DISCUSSION

### Electrochemical behavior of porphyrins

CV curves for  $H_2T(m\text{-OHPh})P$  and  $H_2T(p\text{-OHPh})P$  31 on Pt electrode at negative vs. SCE potentials are shown in Fig. 2. It is evident that the substituent position significantly influences the electrochemical behavior of hydroxyphenyl porphyrins.

In case of  $H_2T(m\text{-OHPh})P$ , three separate reduction waves with a current maximum at potentials around -0.77, -1.16 and -1.55 V are observed. In contrast, in case of  $H_2T(p\text{-OHPh})P$ , there is one more intense oxidation wave. The oxidation peaks are weak at a low scan rate for both porphyrins. The increasing of potential scan rate leads to shifts of reduction peak positions to the negative region (Table 1). The peak currents of the electroreduction waves are proportional to the concentration of both porphyrins. At the same time, the peak current density is proportional to the square root of scan rates of up to 0.05 V/s for both porphyrins as well as oxygen. It indicates the diffusion nature of the electrode processes [26].

In addition, in case of  $H_2T(p\text{-OHPh})P$  the increasing of potential scan rate invokes the appearing of wide oxidation peak in the potential range from -0.8 to -0.2 V. At the same time, there is no redox response if the cycling was in the range from 0.1 to -0.9 V (Fig. 3, curve 2). Thus, we can conclude that the peak is caused by electrooxidation of products formed by the chemical reaction (or structure reorganization) of porphyrin anions.

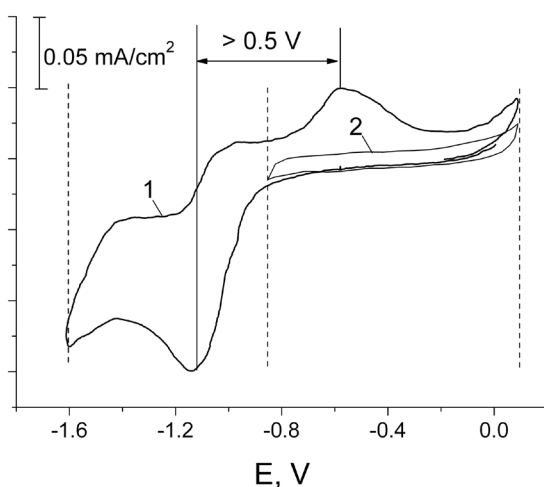
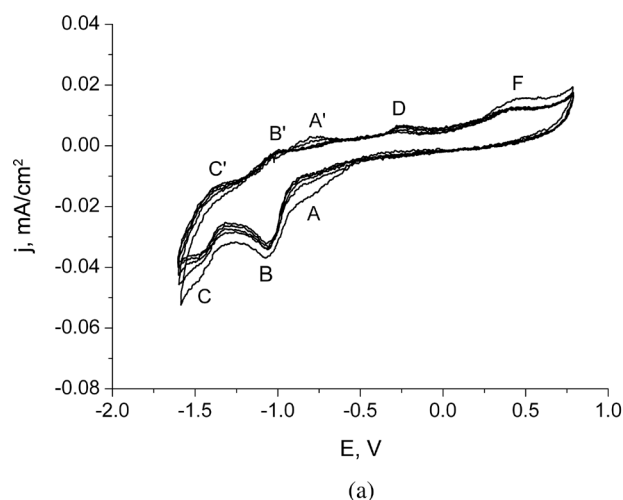


**Fig. 2.** CV response of  $H_2T(m\text{-OHPh})P$  (a) and  $H_2T(p\text{-OHPh})P$  (b) in DMSO during the first cycle at potential scan rates of 0.02, 0.05, 0.1, 0.2, 0.5, 1.0 V/s. The porphyrins concentrations are 1 mM

**Table 1.** Scan rate influence on the reduction waves of H<sub>2</sub>T(*m*-OHPH)P and H<sub>2</sub>T(*p*-OHPH)P

| V <sub>scan</sub> , V/s | H <sub>2</sub> T( <i>m</i> -OHPH)P* |                                       | H <sub>2</sub> T( <i>p</i> -OHPH)P |                                       |
|-------------------------|-------------------------------------|---------------------------------------|------------------------------------|---------------------------------------|
|                         | E <sub>red</sub> , V                | j <sub>red</sub> , mA/cm <sup>2</sup> | E <sub>red</sub> , V               | j <sub>red</sub> , mA/cm <sup>2</sup> |
| 0.01                    | -1.07                               | -0.04                                 | -1.09                              | -0.07                                 |
| 0.02                    | -1.09                               | -0.05                                 | -1.11                              | -0.09                                 |
| 0.05                    | -1.10                               | -0.06                                 | -1.13                              | -0.12                                 |
| 0.1                     | -1.11                               | -0.08                                 | -1.16                              | -0.15                                 |
| 0.2                     | -1.12                               | -0.10                                 | -1.18                              | -0.19                                 |
| 0.5                     | -1.15                               | -0.16                                 | -1.20                              | -0.26                                 |
| 1.0                     | -1.16                               | -0.23                                 | -1.24                              | -0.38                                 |

\*Only the most resolved wave is shown.

**Fig. 3.** Cycling solution of H<sub>2</sub>T(*p*-OHPH)P in the range of: (1) from -1.6 to +0.1; (2) from -0.9 to +0.1 V. The scan rate is 0.1 V/s. The porphyrin concentration of 1 mM**Fig. 4.** CV response of H<sub>2</sub>T(*m*-OHPH)P (a) and H<sub>2</sub>T(*p*-OHPH)P (b) during 5 cycles at potential scan rates of 0.01 V/s. The porphyrin concentrations are 1 mM

The CV curves recorded under the low scan rate (Fig. 4) show that the voltammograms become quite steady during first three cycles. Moreover, some common features were detected in the shape of CV curves. There are three oxidation waves (A, B, C) on the CV cathodic branch which has complementary waves (A', B', C') on the CV anodic branch. The distance between the cathodic and anodic maximums is in the range of 0.07–0.13 V (Table 2) that indicates the quasi reversibility of the charge transfer on the interface in the studied condition.

It should be noted that low intensive waves A, A' probably occurred due to rearrangement phenomena in the adsorbed layer [27, 28]. The slight difference between the voltage of waves in case of *para*- and *meta*-substitutions allows us to make a conclusion about the similarity of charge transfer energy for H<sub>2</sub>T(*m*-OHPH)P and H<sub>2</sub>T(*p*-OHPH)P in DMSO. Therefore, the distinction in the electrochemical behavior of the studied porphyrins should be associated with different kinetics of ion-molecule reactions. Two waves of single electron reductions which accompanied the proton transfer were proposed under negative potentials vs. Fc<sup>0</sup>/Fc<sup>+</sup> [29]. The presence of irreversible oxidation peaks under positive potentials vs. SCE was described elsewhere [30].

For waves B (Fig. 4), the number of electrons involved in the electrochemical step was determined using Equation 1 [31]:

$$\frac{\partial E_p}{\partial(\lg(v))} = \frac{1.15RT}{n\alpha F} \quad (1)$$

where  $v$  is the scan rate;  $E_p$  is the peak voltage,  $F$  is the Faraday constant,  $R$  is the gas constant,  $n$  is the number of electrons involved in electrochemical step,  $\alpha$  is the transfer coefficient. The calculations showed that the value of  $n\alpha$  was around 0.81 for H<sub>2</sub>T(*m*-OHPH)P

**Table 2.** Voltage of cathodic and anodic maxima for the 5th cycle at scan rates of 0.01 V/s. The porphyrin concentration is 1 mM

| Peak label                        | Potential, V |       |       |       |       |       |                |       |
|-----------------------------------|--------------|-------|-------|-------|-------|-------|----------------|-------|
|                                   | A            | A'    | B     | B'    | C     | C'    | D              | F     |
| H <sub>2</sub> T( <i>m</i> -OHP)P | -0.75        | -0.63 | -1.06 | -0.99 | -1.48 | -1.37 | -0.25          | +0.44 |
| H <sub>2</sub> T( <i>p</i> -OHP)P | -0.7         | -0.63 | -1.08 | -0.95 | -1.49 | -1.37 | +0.2<br>(wide) | +0.48 |

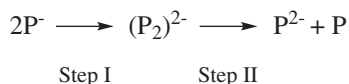
and 0.52 H<sub>2</sub>T(*p*-OHP)P and that the first electron transfer controls the overall reaction rate. In case of H<sub>2</sub>T(*m*-OHP)P, the gaps between peaks B and B' were measured at a different scan rate. After approximation to the zero scan rate the gap between the peaks was about 60 mV. The obtained value confirms the one-electron nature of the redox process. In case of H<sub>2</sub>T(*p*-OHP)P, relation (2) was used.

$$|E_p - E_{p/2}| = 47.7/n\alpha \quad (2)$$

where  $E_{p/2}$  is the half wave voltage.

The calculated  $n\alpha$  value was around 0.5, which also confirms the one-electron nature of wave B.

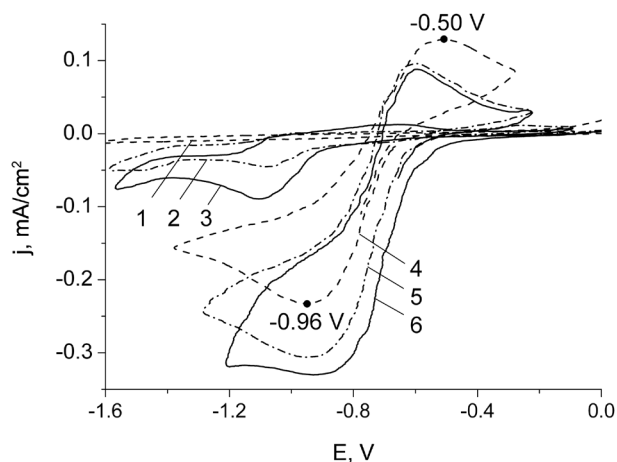
The reduction of compounds including phenolic fragments is often realized *via* multistep proton coupled electron transfer mechanisms [32], so the reduction of the porphyrin under study can be similar. On the other hand, the disproportionation reaction (Scheme 1) is possible because the first reduction peaks (labeled B) demonstrate high current densities [33, 34]. Disproportionation, like most chemical reactions, passes through a transition state (intermediate — two anions are located close enough for the electron transfer ( $P_2$ )<sup>2-</sup>). That intermediate oxidation can be one of possible reasons for peaks appearance in the region from -0.8 to -0.2 V (Fig. 3). The intermediates oxidation will be observed if step II is slow on the voltammetric time scale. One electron waves C (Fig. 4) indicate that step I is slow too. Within this framework, the disparity between H<sub>2</sub>T(*p*-OHP)P and H<sub>2</sub>T(*m*-OHP)P (Fig. 4) current densities indicates a different disproportionation rate of porphyrins.



**Scheme 1.** Disproportionation of porphyrins *via* possible intermediates.

### Effects of porphyrins on O<sub>2</sub>/O<sub>2</sub><sup>•-</sup> redox

The redox response of oxygen in DMSO was described elsewhere [17]. The results (Fig. 5, curve 4) designate the one-electron superoxide (O<sub>2</sub><sup>•-</sup>) ion formation due to well-proven electroreduction reaction in aprotic solvents (Scheme 2) [23, 35]. The calculated values of O<sub>2</sub>/O<sub>2</sub><sup>•-</sup> redox potential and oxygen diffusion coefficient are in

**Scheme 2.** Electrochemical formation of superoxide ion.**Fig. 5.** Cyclic voltammograms: background current (1), H<sub>2</sub>T(*m*-OHP)P (2) and H<sub>2</sub>T(*p*-OHP)P (3) in degassed solution; O<sub>2</sub>/O<sub>2</sub><sup>•-</sup> redox couple without porphyrin (4), with H<sub>2</sub>T(*m*-OHP)P (5), with H<sub>2</sub>T(*p*-OHP)P (6) in oxygen saturated solution. The scan rate is 0.02 V/s. The porphyrin concentrations are 1 mM

good agreement with the data obtained under similar conditions [23, 36–38].

The current density peak of O<sub>2</sub><sup>•-</sup> oxidation shows very good reproducibility and it is significantly higher than the current density peak of porphyrins. The cyclic voltammograms of porphyrins in oxygen-saturated DMSO solutions are shown in Fig. 5, curves 5 and 6. It is clearly seen that porphyrins evoke significant changes in both reduction and oxidation currents. Therefore, the studied porphyrins influence both the synthesis and the decomposition of superoxide ions. The onset potentials for oxygen reduction shift toward the positive region in the porphyrins presence. At the same time, the onset superoxide oxidation in the presence and absence of porphyrin is almost the same. This may indicate that the oxygen reduction is catalyzed by porphyrins, whereas the superoxide oxidation is not catalyzed effectively.

The O<sub>2</sub>/O<sub>2</sub><sup>•-</sup> redox processes were analyzed by the coulometric approach. An example of current *vs.* time plots obtained in the first cycles of voltammograms

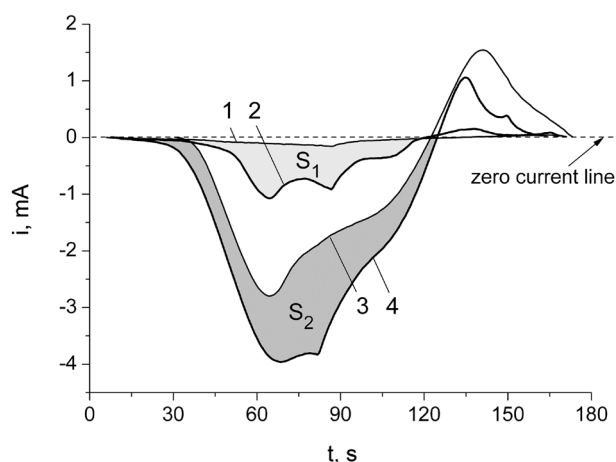


**Fig. 6.** The redox currents vs. time plots: (1) background; (2) 1 mM  $H_2T(p\text{-OHPh})P$  in degassing solution; (3) oxygen in oxygenated solution; (4) porphyrins and oxygen in oxygenated solution. The scan rate is 0.02 V/s

are shown in Fig. 6. The electroreduction process is accompanied by an electron transfer from the electrode to the electroactive species in the solution, so they dominate if the current value is below the zero current line. The quantity of reduction species produced during the first CV cycle is proportional to the quantity of electricity ( $Q$ ) of reduction processes. The  $Q$  values were determined by integrating the experimental  $i(t)$  dependence after correcting the current value using background current.

The gray colored area between the curves labeled 1 and 2 (Fig. 6) corresponds to the quantity of electricity associated with  $H_2T(p\text{-OHPh})P$  electroreduction in the degassing solution ( $Q_{1\text{red}}$  in Table 3). The quantity of electricity  $Q_{2\text{red}}$  associated with oxygen electroreduction in the oxygenated solution and  $Q_{3\text{red}}$  — porphyrins and oxygen electroreduction in the oxygenated solution was determined in a similar way. The gray colored area between the curves labeled 3 and 4 shows the  $Q_{3\text{red}} - Q_{2\text{red}}$  value that should be equal to  $Q_{1\text{red}}$  in case of two independent processes. In other words, the  $Q_{3\text{red}} - Q_{1\text{red}}$  value (the area between the curves labeled 2 and 4) should be equal to  $Q_{2\text{red}}$ . The coulometric characteristics of the reduction processes are presented in Table 3.

According to Table 3, simultaneous reduction processes of porphyrins and oxygen lead to an increase in  $Q_{\text{red}}$  values. So, the charges of individual oxygen reduction ( $Q_{2\text{red}}$ ) differ by more than 15% from the  $Q_{3\text{red}} - Q_{1\text{red}}$  values estimated the charges of oxygen reduction in porphyrins presence if the processes are assumed additive.

Figure 7 illustrates the effects of  $H_2T(m\text{-OHPh})P$  and  $H_2T(p\text{-OHPh})P$  on the redox process of the  $O_2/O_2^{\cdot-}$  couple. In general, the porphyrins evoke a similar transformation of CV curves: the shift of positions of cathodic and anodic maxima as well as a decrease in the reduction onset potentials. The decrease in the gaps between the cathodic and anodic maxima indicates the increasing rate constants of the interfacial electron transfer [31]. The influence of (aminophenyl)porphyrins was similar as described elsewhere [17]. Obviously,

**Table 3.** Coulometric characteristics of reduction processes (scan rate of 0.02 V/s)

| Porphyrin concentration, 1 mM            | Background ( $Q_{0\text{red}}$ , mC) | $Q_{2\text{red}}$ , mC | $Q_{1\text{red}}$ , mC | $Q_{3\text{red}}$ , mC | $Q_{3\text{red}} - Q_{1\text{red}}$ , mC |
|--|--------------------------------------|------------------------|------------------------|------------------------|--|
| <b><math>H_2T(m\text{-OHPh})P</math></b> |                                      |                        |                        |                        |  |
| 0.00                                     | 0.76                                 | 13.19                  | —                      | —                      | 13.19                                    |
| 0.05                                     | 0.76                                 | 13.19                  | 0.69                   | 13.52                  | 12.83                                    |
| 0.10                                     | 0.76                                 | 13.19                  | 1.11                   | 14.3                   | 13.19                                    |
| 0.25                                     | 0.76                                 | 13.19                  | 1.24                   | 15.6                   | 14.36                                    |
| 0.50                                     | 0.76                                 | 13.19                  | 1.82                   | 15.77                  | 13.95                                    |
| 1.00                                     | 0.76                                 | 13.19                  | 2.77                   | 18.92                  | 16.15                                    |
| 1.50                                     | 0.76                                 | 13.19                  | 3.61                   | 21.34                  | 17.73                                    |
| <b><math>H_2T(p\text{-OHPh})P</math></b> |                                      |                        |                        |                        |  |
| 0.00                                     | 0.76                                 | 13.19                  | —                      | —                      | 13.19                                    |
| 0.05                                     | 0.76                                 | 13.19                  | 1.24                   | 16.62                  | 15.38                                    |
| 0.10                                     | 0.76                                 | 13.19                  | 1.37                   | 16.00                  | 14.63                                    |
| 0.25                                     | 0.76                                 | 13.19                  | 1.86                   | 16.41                  | 14.55                                    |
| 0.50                                     | 0.76                                 | 13.19                  | 2.78                   | 18.87                  | 16.09                                    |
| 1.00                                     | 0.76                                 | 13.19                  | 4.39                   | 21.98                  | 17.59                                    |
| 1.50                                     | 0.76                                 | 13.19                  | 6.26                   | 22.44                  | 16.18                                    |

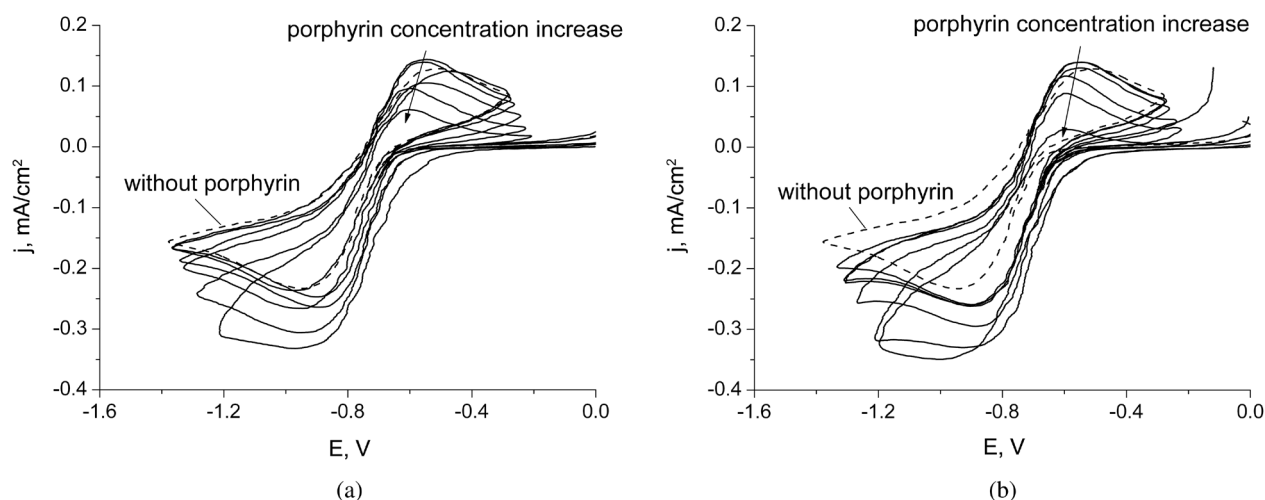


**Fig. 7.**  $\text{H}_2\text{T}(m\text{-OHPh})\text{P}$  (a) and  $\text{H}_2\text{T}(p\text{-OHPh})\text{P}$  (b) influence on the  $\text{O}_2/\text{O}_2^*$  redox process. The scan rate is 0.02 V/s. The porphyrin concentration of 0.00, 0.05, 0.10, 0.25, 0.50, 1.0, 1.5 mM



**Scheme 3.** Electron transfer reaction between superoxide and porphyrin anions.

porphyrins act as redox mediators, most probably, due to  $\text{Por}\cdots\text{O}_2$  and  $\text{Por}\cdots\text{O}_2^*$  adducts formation because of the significant interaction of (hydroxyphenyl)porphyrins with oxygen and superoxide ions that was confirmed by the transfer of excitation [22, 39] and complexation [40] phenomena. The greater values of reduction currents in porphyrins presence can be explained by the reaction described in Scheme 3.

The dimensionless current density  $j/j_0$  of  $\text{O}_2^*$  oxidation was calculated as a ratio of current densities measured at potentials of peak with ( $j$ ) and without ( $j_0$ ) porphyrin. As Fig. 8 shows, the increase in porphyrins concentration leads to nonlinear variation of  $\text{O}_2^*$  dimensionless current density. According to [14], the only linear part of such dependences is used to evaluate antioxidant activity. In case of  $\text{H}_2\text{T}(p\text{-OHPh})\text{P}$ , the concentration range from 0.05 to 1 mM can be used. In case of  $\text{H}_2\text{T}(m\text{-OHPh})\text{P}$ , it is difficult to offer a linear part of the dependence. Using the logarithmic coordinates [16] leads to certain linearization of data. So, the estimation of superoxide scavenging activities of tetra(aminophenyl)porphyrins [17] was successful in terms of binding constants [16]. The influence of antioxidants [13] and porphyrin [41] on the oxygen reduction was also reported. Hence, the noticeable effects of antioxidant on the oxygen reduction and superoxide oxidation currents as well as nonlinearity of current vs. concentration dependences are quite typical.

### Coulometric approach to the superoxide scavenging activity determination

In our opinion, using of coulometric parameters improves the antiradical activity determination in

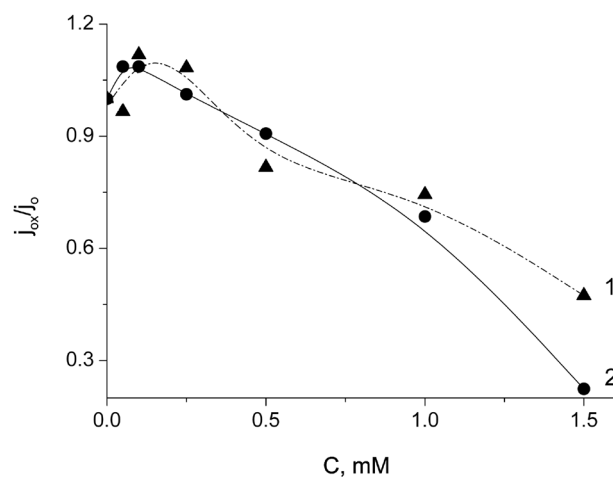


**Fig. 8.**  $\text{H}_2\text{T}(m\text{-OHPh})\text{P}$  (1) and  $\text{H}_2\text{T}(p\text{-OHPh})\text{P}$  (2) influence on dimensionless peak current density of  $\text{O}_2^*$  electrooxidation. The scan rate is 0.02 V/s.  $j_0$  is the peak current density of  $\text{O}_2^*$  electrooxidation without porphyrins

complicated cases. The quantity of electricity of the oxidation processes was calculated by integrating the experimental  $i(t)$  curves of the CV anodic branch. The calculation method was the same as described above: the quantity of electricity of  $\text{O}_2^*$  oxidation in porphyrins presence was estimated as  $Q_{3ox} - Q_{1ox}$  where the quantity of electricity  $Q_{3ox}$  associated with electrooxidation in the oxygenated solution of porphyrins and  $Q_{1ox}$  — with electrooxidation in the degassed solution of porphyrins. The results are shown in Fig. 9.

As it follows from Fig. 9, the coulometric response of superoxide ion vs. porphyrins concentration (line 2) is linear. The lines of  $\text{H}_2\text{T}(m\text{-OHPh})\text{P}$  (a) and  $\text{H}_2\text{T}(p\text{-OHPh})\text{P}$  (b) are extrapolated to the similar zero concentration point. The slopes ( $-2.24 \text{ CM}^{-1}$  for  $\text{H}_2\text{T}(m\text{-OHPh})\text{P}$  and  $-2.95 \text{ CM}^{-1}$  for  $\text{H}_2\text{T}(p\text{-OHPh})\text{P}$ ) indicate more pronounced

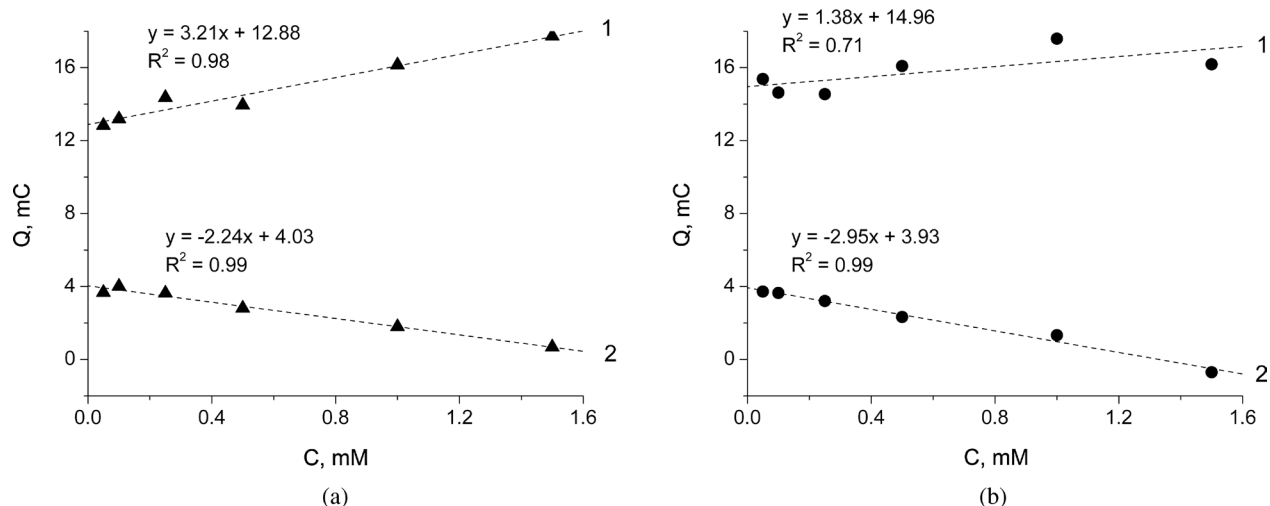


**Fig. 9.**  $H_2T(m-OHPh)P$  (a) and  $H_2T(p-OHPh)P$  (b) influence on the quantity of electricity of  $O_2$  electroreduction (1) and  $O_2^{*+}$  electrooxidation (2)

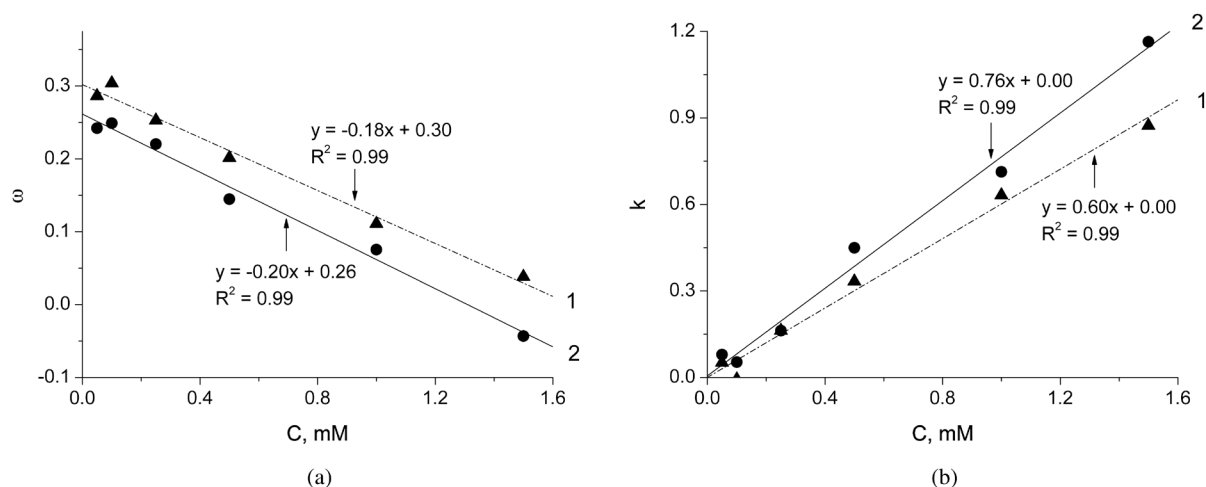


**Fig. 10.** Dimensionless parameters of  $H_2T(m-OHPh)P$  (1) and  $H_2T(p-OHPh)P$  (2) superoxide scavenging activity (explanations are shown in the text)

antioxidant properties of the *para*-substituted compound. But the involvement of porphyrins in the processes of radical synthesis is not considered if only lines 2 are analyzed. As it follows from line 1 Fig. 9 and Table 3, the quantity of electricity of oxygen electroreduction increases almost linearly with porphyrins concentration. So, the factor of superoxide electrosynthesis can be included into the scavenging activity determination.

The dimensionless parameter  $\bar{\omega}$  was calculated using Equation 3:

$$\bar{\omega} = (Q_{3ox} - Q_{1ox}) / (Q_{3red} - Q_{1red}) \quad (3)$$

where  $(Q_{3ox} - Q_{1ox})$  is the quantity of electricity associated with  $O_2^{*+}$  oxidation in porphyrins presence,  $(Q_{3red} - Q_{1red})$  is the quantity of electricity associated with  $O_2$  reduction in porphyrins presence. The  $\bar{\omega}$  values normalize the coulometric response of superoxide (Fig. 10a) and, consequently, improve the radical

scavenging activity determination. The change in the  $\bar{\omega}$  values was described using parameter  $k$  (Equation 4, Fig. 10b).

$$k = (\bar{\omega}_0 - \bar{\omega}) / \bar{\omega}_0 \quad (4)$$

where  $\bar{\omega}_0$  is the  $\bar{\omega}$  value extrapolated to the zero concentration point.

The slopes of  $k$  value vs. concentration plots should be considered as a superoxide scavenging characteristic. The rise of the antioxidant activity leads to an increase in the plot slope. The slopes ( $0.6 \text{ L}\cdot\text{mmol}^{-1}$  for  $H_2T(m-OHPh)P$  and  $0.76 \text{ L}\cdot\text{mmol}^{-1}$  for  $H_2T(p-OHPh)P$ ) show the higher superoxide scavenging properties of  $H_2T(p-OHPh)P$ .

## CONCLUSION

The electrochemical assay of superoxide scavenging activity was adopted to porphyrins having an intricate

electrochemical behavior and a significant effect on the redox of the  $O_2/O_2^{\cdot -}$  couple. The factor of superoxide electro-synthesis included into the scavenging activity determination allows us to obtain the more careful parameter of the radical scavenging activity. The new method was used to demonstrated the hydroxy-group positions influence on the superoxide scavenging activity; it was found to be identical to amino-group positions influence described elsewhere [17]. This fact indicates the similar (hydrogen atom transfer) antioxidant mechanism. Therefore, predominantly effect of bond dissociation energy (BDE) for labile H-atom in phenyl substituents on the antioxidant activities of tetraphenyl porphyrins should be expected.

### Acknowledgements

The authors thank Professor Semeikin A. S. (Ivanovo State University of Chemistry and Technology) for developing methods of porphyrins synthesis and assistance. The research was financially supported by the Russian Foundation for Basic Research, grant no. 13-03-00087.

### REFERENCES

- Ames BN, Shigenaga MK and Hagen TM. *Proc. Natl. Acad. Sci. USA* 1993; **90**: 7915–7922.
- Datta K, Sinha S and Chattopadhyay P. *The National Medical Journal of India* 2000; **13**: 304–310.
- Abreu R, Falcro S, Calhelha RC, Ferreira ICFR, Queiroz M-JRP and Vilas-Boas M. *J. Electroanal. Chem.* 2009; **628**: 43–47.
- Amic D and Lucic B. *Bioorganic & Medicinal Chemistry* 2010; **18**: 28–35.
- Antonova NA, Osipova VP, Kolyada MN, Movchan NO, Milaeva ER and Pimenov YT. *Macroheterocycles* 2010; **3**: 139–144.
- Kuzmin SM, Chulovskaya SA and Parfenyuk VI. *Macroheterocycles* 2013; **6**: 334–339.
- Kasugai N, Murase T, Ohse T, Nagaoka S, Kawakami H and Kubota S. *J. Inorg. Biochem.* 2002; **91**: 349–355.
- Iranzo O. *Bioorg. Chem.* 2011; **39**: 73–87.
- Milaeva ER, Shpakovsky DB, Gracheva YA, Orlova SI, Maduar VV, Tarasevich BN, Meleshonkova NN, Dubova LG and Shevtsova EF. *Dalton Trans.* 2013; **42**: 6817–6828.
- Wasbotten IH, Conradie J and Ghosh A. *J. Phys. Chem. B* 2003; **107**: 3613–3623.
- Apak R, Gorinstein S, Böhm V, Schaich KM, Özyürek M and Güçlü K. *Pure Appl. Chem.* 2013; **85**: 957–998.
- Wei Y, Ji X, Dang X and Hu S. *Bioelectrochemistry* 2003; **61**: 51–56.
- Korotkova EI, Karbainov YA and Avramchik OA. *Analytical and Bioanalytical Chemistry* 2003; **375**: 465–468.
- Bourvellec Le, Hauchard D, Darchen A, Burgot J-L and Abasq M-L. *Talanta* 2008; **75**: 1098–1103.
- Ying-liang W, Xue-ping D and Sheng-shui Hu. *Wuhan University Journal of Natural Sciences* 2003; **8**: 866–870.
- Safeer A and Faria S. *Czech J. Food Sci.* 2012; **30**: 153–163.
- Kuzmin SM, Chulovskaya SA and Parfenyuk VI. *J. Porphyrins Phthalocyanines* 2014; **18**: 585–593.
- Milgrom LR. *J. Chem. Soc, Perkin Trans. I.* 1983; 2535–2539.
- Syrbu SA and Semeykin AS. *Zhurn. Org. Khim.* 1999; **35**: 1262–1265 (in Russian).
- Semeikin AS, Koifman OI and Berezin BD. *Chemistry of Heterocyclic Compounds* 1986; **22**: 629–632.
- Rumyantseva VD, Gorshkova AS and Mironov AF. *Macroheterocycles* 2013; **6**: 59–61.
- Rojkiewicz M, Kus P, Kozub P and Kempa M. *Dyes Pigm.* 2013; **99**: 627–635.
- Sawyer DT and Roberts JL. *J. Electroanal. Chem.* 1966; **12**: 90–101.
- Emmerich W and Rubin B. *Chem. Rev.* 1973; **73**: 1–9.
- Taylor SR and Scribner LL. *The measurement and correction of electrolyte resistance in electrochemical tests*, American Society for Testing and Materials: Philadelphia, 1990.
- Randles JEB. *Trans. Faraday Soc.* 1948; **44**: 327–338.
- Ye T, He Y and Borguet E. *J. Phys. Chem. B* 2006; **110**: 6141–6147.
- Hassani SS, Kim Y-G and Borguet E. *Langmuir* 2011; **27**: 14828–14833.
- Aguilera EN, Jerez LMB and Alonso JL. *Electrochimica Acta* 2013; **98**: 82–87.
- Fagadar-Cosma G, Fagadar-Cosma E, Popa I and Taranu I. *Chem. Bull. "POLITEHNICA" Univ. (Timișoara)* 2007; **52**: 109–112.
- Bard AJ and Faulkner LR. *Electrochemical methods: fundamentals and applications*, John Wiley and Sons, Inc.: New York, 2001.
- Costentin C, Robert M, Saveant J-M. *Chem. Rev.* 2010; **110**: PR1–PR40.
- Mastragostino M, Nadjo L and Saveant J-M. *Electrochim. Acta* 1968; **13**: 721–749.
- Gupta N and Linschitz H. *J. Am. Chem. Soc.* 1997; **119**: 6384–6391.
- Fujinaga T, Isutsy K and Adachi T. *Bull. Chem. Soc. Jap.* 1969; **42**: 140–145.
- Tsushima M, Tokuda K and Ohsaka T. *Anal Chem.* 1994; **66**: 4551–4556.

37. Laoire CO, Mukerjee S, Abraham KM, Plichta EJ and Hendrickson MA. *J. Phys. Chem.* 2010; **114**: 9178–9186.
38. *Handbook of Electrochemistry*, Zoski CG. (Ed.) Elsevier: Amsterdam Boston Heidelberg London New York Oxford Paris San Diego San Francisco Singapore Sydney Tokyo, 2007.
39. Ding H, Yu H, Dong Y, Tian R, Huang G, Boothman DA, Sumer BD and Gao J. *J. Control Release* 2011; **156**: 276–280.
40. De Luca G, Romeo A and Scolaro LM. *J. Phys. Chem. B* 2006; **110**: 14135–14141.
41. Popov I, Kyzmin S, Chulovskaya S, Semeikin A and Parfenyuk V. *Macroheterocycles* 2012; **5**: 131–135.